EXPERIMENTS WITH SMALL UAS TO SUPPORT SAR TOMOGRAPHIC MISSION FORMULATION

Brian Hawkins[1], *Matthew Anderson*[2], *Sam Prager*[1,3], *Soon-Jo Chung*[1,2], *and Marco Lavalle*[1]

[1]Jet Propulsion Laboratory, California Institute of Technology, Pasadena, CA, USA
[2]California Institute of Technology, Pasadena, CA, USA
[3]University of Southern California, Los Angeles, CA, USA

ABSTRACT

The advent of smaller SAR satellites and cheaper access to space is bringing the notion of a multistatic SAR constellation into the realm of feasibility. Researchers at JPL are studying a Distributed Aperture Radar Tomographic Sensors (DARTS) mission concept intended to measure Earth's surface topography and vegetation using TomoSAR techniques. This paper describes progress on the airborne testbed for the DARTS study. The testbed is the union of a software-defined radio that implements a radar and synchronization link together with a small uninhabited aerial system (sUAS) that serves as a platform with precise control of the observation geometry. Initial experiments have demonstrated successful multi-sensor synchronization as well as acquisition and processing of monostatic SAR imagery.

Index Terms— Synthetic Aperture Radar, SAR, sUAS

1. INTRODUCTION

Synthetic aperture radar (SAR) is now a well-known technique for all-weather imaging with foliage-penetrating capabilities [1]. These aspects make SAR well suited for remote sensing of forests, whose properties like biomass are important climate variables [2]. The relatively recent developments in SAR tomography [3] extend the synthetic aperture in the cross-track direction and enable three-dimensional volumetric imaging throughout the forest canopy. ESA's upcoming BIOMASS satellite mission will include a tomographic component with exactly this goal in mind [4, 5].

While the collection of tomographic data from a single, monostatic SAR satellite is a novel and exciting prospect, such measurements will inevitably suffer from temporal decorrelation as the cross-track aperture must be synthesized over several weeks or months. The temporal decorraltion could be mitigated by acquiring simultaneous observations from multiple platforms, a technique successfully demonstrated by the TanDEM-X mission [6]. The advent of modestly-sized SAR platforms like ICEYE [7] and Capella [8] together with the proliferation of increasingly affordable launch options raises the possibility that a constellation of sensors might one day achieve multistatic tomographic measurements at reasonable cost.

Towards that end, we have begun evaluating a Distributed Aperture Radar Tomographic Sensors (DARTS) mission concept. A high-level description of this activity is the subject of a companion paper [9]. In order to investigate and verify various aspects of the mission architecture, we are developing an airborne component using a software-defined radio (SDR) mounted on small uninhabited aerial system (sUAS). This paper discusses the initial system design, experiments, and data processing of the DARTS sUAS testbed.

2. HARDWARE

A quadrotor designed and built at Caltech is used as the sUAS platform (Fig. 1). The sUAS has a payload capacity of 1.5 kg and can operate at a maximum speed of 15 m/s. On-board state estimation using the flight controller (APM:Copter) fuses IMU, barometric, differential GPS, optical flow and LIDAR measurements to provide an accurate estimate of the sUAS's position in real-time. Additionally, raw GPS pseudo-range and Doppler measurements are logged, enabling high-precision orbit and clock solutions to be used to improve the position estimate of in post-processing.

The radar is implemented using an Ettus USRP E312 COTS software defined radio (SDR). The USRP E312 is a 2x2 MIMO unit with up to 50 MHz instantaneous bandwidth selectable in the range 70 MHz to 6 GHz. For these experiments, it was configured for operations at L-band and S-band, like NISAR [10]. The unit contains an RF tranceiver and a Xilinx Zynq 7020 SoC with an FPGA and ARM CPU for both hardware and software programmability. The antennas are mounted on the ends of a 1.2 m carbon fiber boom that is rigidly attached to the top of the UAS.

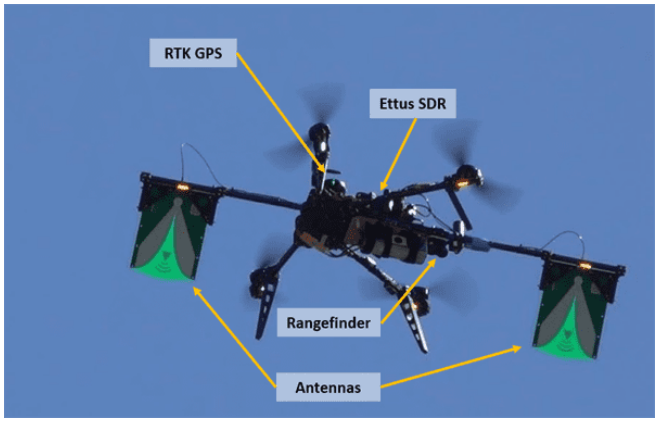

Fig. 1. sUAS for investigating techologies relevant to SAR tomography.

3. PROCESSING

One of the key challenges in any multistatic SAR system is synchronization of the signal across sensors with independent local oscillators. Left uncompensated, synchronization errors can cause poor focusing, increased sidelobes, geometric distortions, and phase errors [11]. For these experiments we employ the synchronization link recently described in [12]. The link involves coarse synchronization using a GPS PPS signal and fine synchronization via the broadcast of $2N$ messages in TDMA fashion to synchronize a network of N sensors. This scheme results in better than 1 ns precision in terms of baseband clock offset, carrier phase, and pairwise time of flight.

A particular difficulty for airborne SAR systems is the irregular platform trajectory, which violates the azimuth-invariance assumptions typical of efficient processing algorithms. Since throughput is not a concern, we simply use a time-domain backprojection algorithm to focus the data in azimuth [13]. That is, we integrate the synthetic aperture independently for each illuminated target while compensating the delay and associated carrier phase. In the monostatic case the delay is $2R(t)/c$ while in the multistatic case it is $(R_{TX}(t) + R_{RX}(t))/c$ where the subscripts denote transmit and receive. The distance R is calculated at each pulse time t using the measured platform location and the fixed target position.

4. INITIAL EXPERIMENTS

Our experimental campaign proceeds in incremental stages, with initial tests intended to characterize performance of the SDR radar and sUAS platform independently. The sUAS was operated at an RC aircraft range in Duarte, California, in order to assess its flight performance. Its ability to follow a predetermined path is directly relevant to future tomographic studies where we will desire a specific distribution of interferometric baselines. The result of its attempt to follow programmed waypoints is shown in Fig. 2, with tracking errors generally at decimeter level.

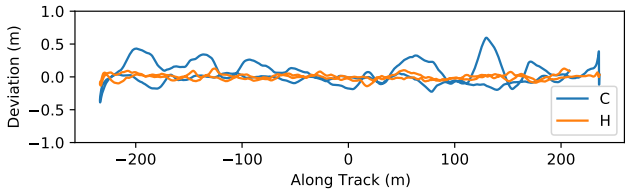

Fig. 2. Flight performance of the sUAS platform. Cross-track (C) and vertical (H) offsets from a straight-line trajectory are well under 1 m.

A trio of tripod-mounted SDR units were operated at the same location in order to assess the performance of the synchronization link. The first configuration was a static triangle with roughly 10 m separation between units as shown in Fig. 3. Since they are not moving, the distribution of relative time-of-flight (TOF) measurements indicates the precision of the clock synchronization. Histograms of the TOF between units is shown in Fig. 4. The standard deviation of the TOF estimates was on the order of 0.1 ns, consistent with results reported in [12].

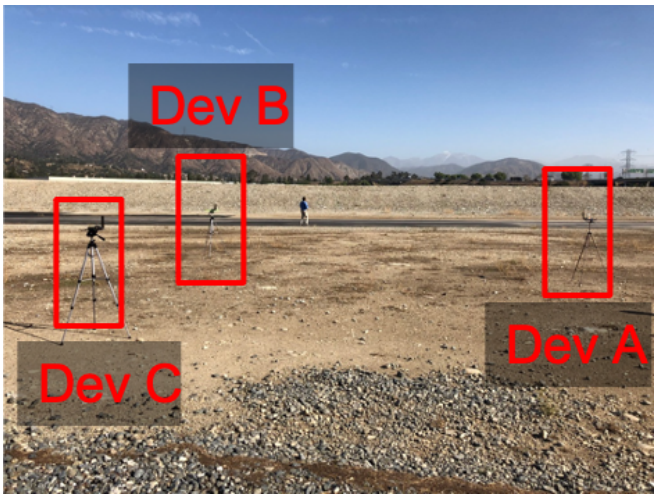

Fig. 3. Synchronized time-of-flight experimental setup for three stationary SDR units separated by 10 m.

The second SDR test involved a similar configuration, except one of the units was repositioned every 60 seconds in order to characterize performance over a variety of distances up to $\sim$ 280 m. The roving unit was moved in $\sim$ 40 m step intervals as shown in Fig. 5. The mean and standard deviation with respect to each interval is given in Fig. 6. As expected, synchronization accuracy tended to degrade with increasing distance (decreasing SNR), though the TOF standard deviation remained below 1 ns at all distances. Furthermore, the

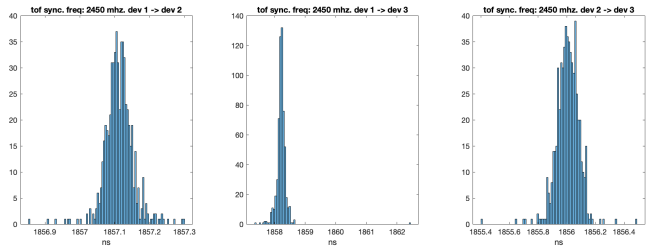

Fig. 4. Histograms of the time-of-flight measured between three stationary SDR units separated by 10 m, demonstrating clock synchronization better than 1 ns.

experiment was conducted at 2.4 GHz RF frequency in the presence of numerous high-power RC aircraft transmitters, which were measured to be operating at the same frequency. In some cases, the interfering noise fully saturated the radar receiver. Interference from RC aircraft in close proximity further degraded SNR and even caused occasional problems decoding the QPSK messages at longer ranges. This motivated the addition of error correcting codes in the radar software.

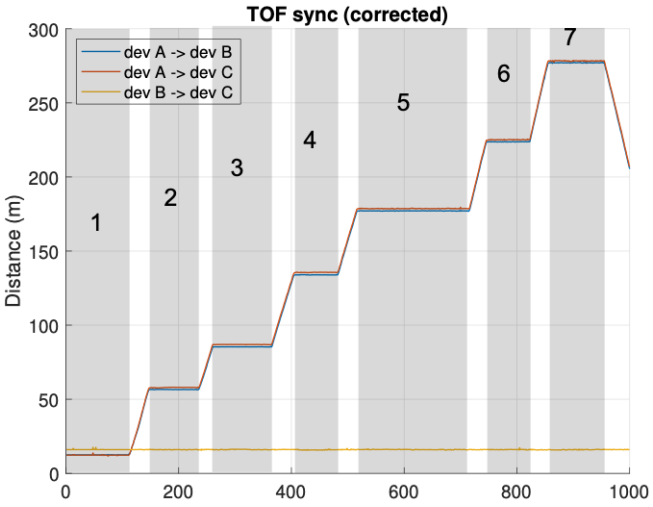

Fig. 5. Time of flight measured between SDR units where one (device A) is roving.

5. AIRBORNE SAR EXPERIMENTS

UAV flight experiments using the Ettus SDR payload were carried out at Caltech athletic fields. Four trihedral corner reflectors were placed on the south field and surveyed using a ublox F9P RTK GPS and PPK position estimation to aid geometric calibration and focusing.

The UAS was automatically commanded to fly along multiple tracks (100 m length, 110 m altitude, 4 m offsets) perpendicular to the corner reflector boresight, giving a slant range of between 200 m and 250 m (Fig. 7). The transmit

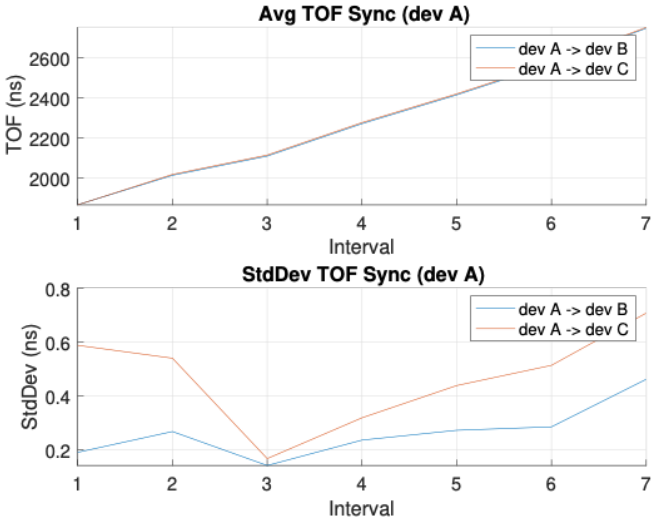

Fig. 6. Interval statistics for time of flight measured between SDR units where one (device A) is roving demonstrating sub-1 ns performance.

and receive antennas were mounted side-looking and rotated 60° off nadir. The SDR achieved a 27 Hz mean effective pulse repetition frequency in its 85 MHz L-band configuration, so airspeed was limited to 1-2 m/s in order to maintain adequate azimuth spectral sampling. A total of seven flights were completed over 35 minutes of flying time.

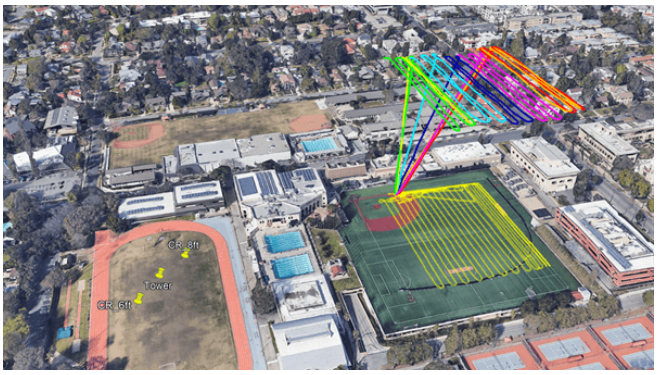

Fig. 7. Google Earth overlay of the seven flights completed, along with the locations of the corner reflectors. The ground trace of the UAS is shown in yellow on the field.

The position and attitude of the UAS was stored on-board at 35 Hz and used to reconstruct the position of each of the antennas in post-processing. Since there was no direct communication between the radar and UAS, the position data was interpolated to the radar pulse times using GPS timestamps measured independently by each subsystem.

Fig. 8 shows the focused SAR image formed by a single pass on one of the flights. In this case, processing with telemetry alone did not result in full azimuth resolution, so

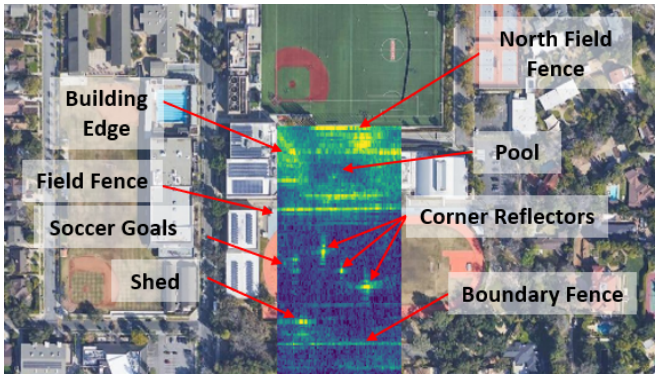

Fig. 8. Monostatic SAR image collected from a single pass during the flights.

additional autofocus corrections were derived from measurements of the corner reflectors made in the range-compressed data, similar to [14, 15]. Afterwards all calibration targets are visible and several interesting features can be discriminated.

6. CONCLUSION

The DARTS project has demonstrated capabilities for precision navigation and multi-platform synchronization that are essential stepping stones towards its goal of realizing a tomographic SAR system. Furthermore, it recently achieved a "first light" monostatic SAR image with encouraging results. Future work includes characterization of SAR performance metrics and interferometric processing.

7. REFERENCES

[1] I. Woodhouse, *Introduction to Microwave Remote Sensing*, Chapman and Hall/CRC, Boca Raton, 2017.

[2] H. H. Shugart, S. Saatchi, and F. G. Hall, "Importance of structure and its measurement in quantifying function of forest ecosystems," *Journal of Geophysical Research: Biogeosciences*, vol. 115, no. G2, June 2010.

[3] A. Reigber and A. Moreira, "First demonstration of airborne SAR tomography using multibaseline L-band data," *IEEE Transactions on Geoscience and Remote Sensing*, vol. 38, no. 5, pp. 2142–2152, 2000.

[4] K. Scipal, M. Arcioni, J. Chave, J. Dall, F. Fois, T. LeToan, C. Lin, K. Papathanassiou, S. Quegan, F. Rocca, S. Saatchi, H. Shugart, L. Ulander, and M. Williams, "The BIOMASS mission — an ESA Earth Explorer candidate to measure the BIOMASS of the earth's forests," in *2010 IEEE International Geoscience and Remote Sensing Symposium*, 2010, pp. 52–55.

[5] D. Ho Tong Minh, S. Tebaldini, F. Rocca, T. Le Toan, L. Villard, and P. C. Dubois-Fernandez, "Capabilities of biomass tomography for investigating tropical forests," *IEEE Transactions on Geoscience and Remote Sensing*, vol. 53, no. 2, pp. 965–975, 2015.

[6] G. Krieger, A. Moreira, H. Fiedler, I. Hajnsek, M. Werner, M. Younis, and M. Zink, "TanDEM-X: A satellite formation for high-resolution SAR interferometry," *IEEE Transactions on Geoscience and Remote Sensing*, vol. 45, no. 11, pp. 3317–3341, 2007.

[7] ICEYE, "Iceye: Your choice for persistent monitoring," `https://www.iceye.com`.

[8] G. Farquharson, W. Woods, C. Stringham, N. Sankarambadi, and L. Riggi, "The Capella synthetic aperture radar constellation," in *EUSAR 2018; 12th European Conference on Synthetic Aperture Radar*, 2018, pp. 1–5.

[9] M. Lavalle, I. Seker, J. Ragan, E. Loria, R. Ahmed, B. P. Hawkins, S. Prager, D. Clark, R. Beauchamp, M. Haynes, P. Focardi, N. Chahat, M. Anderson, K. Matsuka, V. Capuano, and S.-J. Chung, "Distributed aperture radar tomographic sensors (DARTS) to map surface topography and vegetation structure," in *2021 IEEE International Geoscience and Remote Sensing Symposium*, July 2021.

[10] P. Rosen, S. Hensley, S. Shaffer, W. Edelstein, Y. Kim, R. Kumar, T. Misra, R. Bhan, R. Satish, and R. Sagi, "An update on the NASA-ISRO dual-frequency DBF SAR (NISAR) mission," in *2016 IEEE International Geoscience and Remote Sensing Symposium*, 2016, pp. 2106–2108.

[11] G. Krieger and M. Younis, "Impact of oscillator noise in bistatic and multistatic SAR," *IEEE Geoscience and Remote Sensing Letters*, vol. 3, no. 3, pp. 424–428, 2006.

[12] S. Prager, M. S. Haynes, and M. Moghaddam, "Wireless subnanosecond RF synchronization for distributed ultrawideband software-defined radar networks," *IEEE Transactions on Microwave Theory and Techniques*, vol. 68, no. 11, pp. 4787–4804, 2020.

[13] O. Frey, C. Magnard, M. Ruegg, and E. Meier, "Focusing of airborne synthetic aperture radar data from highly nonlinear flight tracks," *IEEE Transactions on Geoscience and Remote Sensing*, vol. 47, no. 6, pp. 1844–1858, 2009.

[14] M. Lort, A. Aguasca, C. López-Martínez, and T. M. Marín, "Initial evaluation of SAR capabilities in UAV multicopter platforms," *IEEE Journal of Selected Topics in Applied Earth Observations and Remote Sensing*, vol. 11, no. 1, pp. 127–140, 2018.

[15] D. Henke, M. Frioud, J. Fagir, S. Guillaume, M. Meindl, A. Geiger, S. Sieger, D. Janssen, F. Klöppel, M. Caris, S. Stanko, M. Renker, and P. Wellig, "Miranda35 experiments in preparation for small UAV-based SAR," in *2019 IEEE International Geoscience and Remote Sensing Symposium*, 2019, pp. 8542–8545.